# Molecular modeling of membrane modifications after exposure to nanosecond, pulsed electric fields

P. Thomas Vernier[*a,b]
[a]Ming Hsieh Department of Electrical Engineering, Viterbi School of Engineering, University of Southern California, Los Angeles, CA, USA
[b]Frank Reidy Research Center for Bioelectrics, Old Dominion University, Norfolk, VA, USA

## ABSTRACT

Structural modifications of cell membranes are among the primary consequences of exposure to intense nanosecond pulsed electric fields. These alterations can be characterized indirectly by monitoring changes in electrical conductance or small molecule permeability of artificial membranes or suspensions of living cells, but direct observations of the membrane-permeabilizing structures remain out of the reach of experiments. Molecular dynamics simulations provide an atomically detailed view on the nanosecond time scale of the sequence of events that follows the application of an external electric field to a system containing an aqueous electrolyte and a phospholipid bilayer, a simple approximation of a cell membrane. This biomolecular perspective, which correlates with experimental observations of electroporation (electropermeabilization) in many respects, points to the key role of water dipoles, driven by the electric field gradients at the membrane interface, in the initiation and construction of the membrane defects which evolve into conductive pores. We describe a method for stabilizing these lipid electropores in phospholipid bilayers, and for characterizing their stability and ion conductance, and we show how the properties of these nanoscale structures connect with continuum models of electroporation and with experimental results.

**Keywords**: electropermeabilization, electroporation, electropore, molecular dynamics, water bridge, pore stabilization

## 1. INTRODUCTION

### 1.1 Reorganization of interfacial water dipoles

Electroporation, also known as electropermeabilization, is the process leading to an increase in membrane permeability that follows an appropriate exposure of cells to an external electric field. Through a mechanism not completely understood, permeabilizing structures appear in the membrane, enabling the normally blocked transport of ions and small molecules into and out of the cell[1-3]. Electroporation is widely used in biotechnology and medicine, from drug and gene delivery into cells in the laboratory to tumor therapy in the clinic[4-8]. Despite these broad applications the details of the molecular mechanisms of electropore creation in living cells are not well understood[9].

Direct experimental observation of electropermeabilization is difficult because of the small spatial and fast temporal scales of this process. This has spurred the development of theoretical models to facilitate the interpretation of experimental data. Continuum models[10,11] represent electroporation reasonably well at the macro scale, but they contain a number of empirically fitted parameters and cannot describe the detailed structural reorganization of the membrane at the various stages in the lifetime of an electropore: initiation, growth, and decay. Molecular dynamics (MD) simulations, although limited in the physical size of the system by computational constraints, provide atomic detail of the processes of pore creation and annihilation.

### 1.2 Nanoscale permeabilization

Single electric pulses can permeabilize cell membranes in less than 10 ns[12-15]. Experimental data and MD simulations are consistent with a process in which an external electric field facilitates the construction of a transmembrane water bridge, followed by phospholipid head group migration into the membrane interior and the establishment of a nanometer-diameter, hydrophilic pore.

MD studies have shown from the beginning that interfacial water dipoles are critical components of the initiation and growth of the membrane defects that lead to electropore formation[16], and it is becoming clear that the electric field-driven reorganization of water dipoles is the process that drives electroporation.

Terahertz and Ultrashort Electromagnetic Pulses for Biomedical Applications, edited by Gerald J. Wilmink, Bennett L. Ibey,
Proc. of SPIE Vol. 8585, 85850D · © 2013 SPIE · CCC code: 1605-7422/13/$18 · doi: 10.1117/12.2005996

A mechanism for electropore formation consistent with our simulations begins with a bias in the random thermal motions of water and head group dipoles in the interface, driven by the applied electric field, leading to intrusions of water into the bilayer interior[17]. This intrusive water forms a yet to be identified water "pedestal", either as the defect is formed or as a consequence of the continued interaction of the reorganizing water (and lipids) with the electric field. This structure provides a platform for the construction of a chain of water that eventually bridges the membrane.

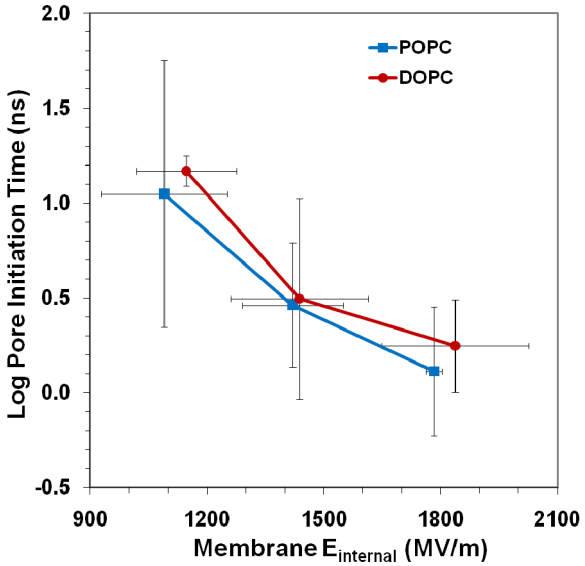


Figure 1. Electropore initiation time is a nonlinear function of the magnitude of the porating electric field. Pore initiation time is exponentially dependent on the applied electric field, expressed here as the electric field observed in the lipid bilayer interior in molecular dynamics simulations. Error bars are standard error of the mean from at least three independent simulations. Data are from Tables 4 and 5 of [Levine and Vernier, JMB, 2010].

Figure 1 shows pore initiation time (time between application of porating electric field and the appearance of a membrane-spanning water column as a function of the electric field magnitude[18]. The exponential decrease in initiation time with increased electric field indicates a field-driven reduction in the activation energy for pore formation.

Simulation results like this connect molecular dynamics representations with analytical and numerical models and with experimental observations. For example, the relation between electric field and pore creation rate is described in the stochastic pore model in the following expression,

$$K_{pore} = Ae^{-E(r,V_m)/k_BT}, \qquad (1)$$

where $K_{pore}$ is the pore creation rate, $A$ is a rate constant, $E(r,V_m)$ is the energy of a pore with radius $r$ at transmembrane potential $V_m$, and $k_B$ and $T$ are the Boltzmann constant and the absolute temperature[19-22].

### 1.3 Properties of individual lipid electropores

A new method for stabilizing lipid electropores in MD simulations[23-25] allows us to study these permeabilizing structures in a steady-state, quasi-equilibrium. The pores are maintained in a stable condition by applying a sustaining electric field across the membrane. The diameter of the pore is a function of the field magnitude, and with this technique we can systematically characterize the conductance of single electropores. Here we compare experimental ion conductance values for single pores[26-28] with those obtained from our simulations of field-stabilized electropores in 1-palmitoyl-2-oleoyl-*sn*-glycero-3-phosphatidylcholine (POPC) bilayers.

## 2. METHODS

### 2.1 Molecular dynamics simulations

Unless otherwise indicated all simulations were performed as described in[29]. Systems contain a bilayer composed of 128 POPC lipids (64 per leaflet) and approximately 9000 water molecules (~70 waters/lipid), corresponding to an initial system box size of approximately 7 nm × 7 nm × 10 nm. The GROMACS function 'genion' was used to replace bulk water molecules with $Na^+$, $K^+$, and $Cl^-$. 40 $Na^+$ and 40 $Cl^-$ were added to the NaCl system and 22 $K^+$ and 22 $Cl^-$ were added to the KCl system in order to create systems with free ion concentrations close to physiological values after equilibration. A custom Perl program was used to check the binding of ions to the lipid bilayer; an ion within 0.3 nm of a POPC glycerol backbone acyl oxygen is considered bound. We equilibrate the systems until the numbers of free and bound ions in the system and the area per lipid reach a steady value. Equilibration time is typically 100 ns for NaCl systems and 50 ns for KCl systems.

### 2.2 Conductance simulations

To produce electric field-stabilized pores[25], we apply an external porating electric field (400 MV/m) to a POPC bilayer. When the phosphorus groups from the top and bottom leaflets merge, and the pore radius reaches approximately 1 nm, we reduce the external field to a lower, sustaining field to maintain the pore in a steady state. Ions in the system are electrophoretically driven through the pore, creating a current. Conductance simulations were run for 100 ns after the pore stabilization. Three independent trials were carried out for each condition.

### 2.3 Pore radius measurement, current measurement, and conductance calculation

Pore radius, current, and conductance are extracted from conductance simulation trajectories using custom algorithms described elsewhere.

### 2.4 Images

Molecular graphics images were generated with Visual Molecular Dynamics (VMD).

## 3. RESULTS AND DISCUSSION

### 3.1 Water bridges in lipid bilayers and in vacuum

Electropore creation (Fig. 2) begins with a water intrusion into the bilayer interior (Fig. 2B). In the presence of an electric field these interface defects are extended until they form a bridge (Fig. 2C) lined by phospholipid head groups. Water molecules always lead this process, followed by the phospholipid head groups. What drives water, a highly polar compound, to form these chains across the apolar environment of the membrane interior?

We have noted similarities between electropore formation in lipid bilayers and electric field-enhanced evaporation of water (electroevaporation). The nanoscale structures that nucleate the electric field-enhanced evaporation of water[30] look like the cones of intruding water that we observe in our simulations (Fig. 2B). In an investigation of these similarities we demonstrated the primary role of interfacial water in the electroporation process by constructing systems in which a 4 nm vacuum gap (distance from interface to interface in a typical phospholipid bilayer) separates two regions of bulk water. These systems are stable over the tens of nanoseconds of our simulations. But when an electric field is applied, the system "porates" (Fig. 3). Water intrudes into the vacuum (Fig. 3B), extends across the gap (Fig. 3D, 3E), and then expands into a larger "pore" (Fig. 3F). This rearrangement of interfacial water is very much like what happens to water in the formation of a lipid electropore (Fig. 2).

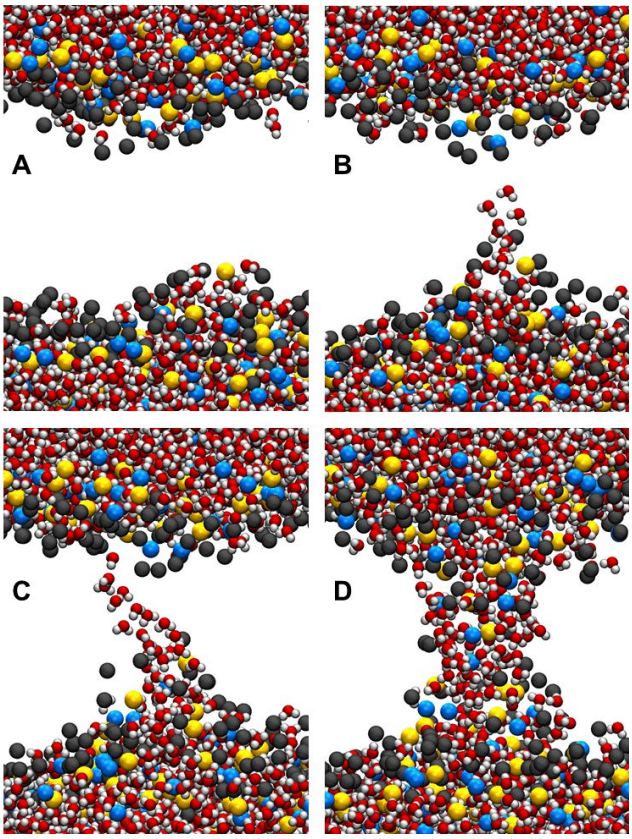


Figure 2. Electropore creation (A) Molecular dynamics representation of a POPC bilayer. Small red and white spheres at the top and bottom of the panel are water oxygen and hydrogen atoms. Gold and blue spheres are head group phosphorus and nitrogen, respectively, and large gray spheres are phospholipid acyl oxygens. The hydrocarbon chains in the interior of the bilayer are not shown. In the presence of a porating electric field, a water intrusion appears (B) and extends across the bilayer (C). Head groups follow the water to form a hydrophilic pore (D). The time from water bridge initiation to the formation of the head-group-lined pore is less than 5 ns.

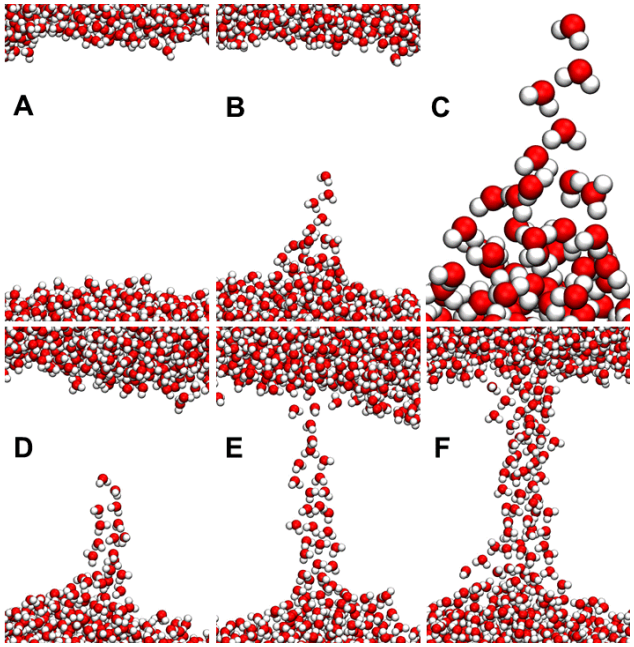


Figure 3. Formation of a water bridge across a vacuum gap separating two regions of liquid water. Snapshots from 621 ps (A), 645 ps (B), 661 ps (D), 673 ps (E), and 683 ps (F) after application of a 900 MV/m electric field. A magnified view of the water bridge precursor structure (C), shows the alignment of the water dipoles in the electric field (directed downward).

### 3.2 Na+, K+, and Cl- conductance

Lipid electropore conductance is determined by the native ion conductance, by ion-pore interactions, and by the radius of the pore, which can be controlled with the external electric field $E_s$. Ion conductance increases with pore radius, as one would expect, but $Na^+$ conductance is less than $K^+$ conductance for a given radius. This is a consequence of stronger $Na^+$ binding to the interface, which results also in the nonlinear relation between pore radius and $Na^+$ conductance at small values for the pore radius (Figure 4). At $r_{pore}$ = 0.77 nm (the smallest pore radius measured in the KCl system), the ratio of the cation conductances, $G_K/G_{Na}$, is approximately 5.6, a reflection of the stronger interaction between $Na^+$ and the phospholipid head groups in the pore wall relative to $K^+$. At $r_{pore}$ = 1.5 nm (the largest pore radius measured in the NaCl system), $G_K/G_{Na}$ is only 2.3. As the pore size increases a larger and larger fraction of the sodium ions traversing the pore sees only bulk-like water and is not slowed by pore wall binding, thus the $Na^+$ conductance increases relative to the $K^+$ conductance and $G_K/G_{Na}$ decreases. Preliminary data shows that this ratio approaches 1.8, the value in bulk water simulations, as the pore radius increases. $K^+$ and $Cl^-$ interact very little with the pore wall; their conductances in lipid electropores are similar to those in bulk water.

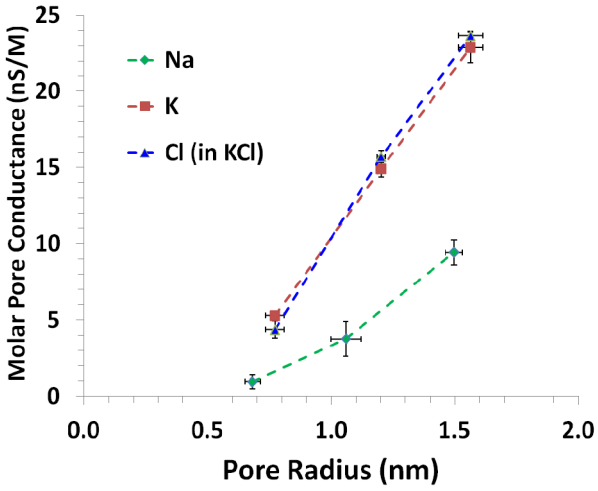


Figure 4. $Na^+$ and $K^+$ conductance versus pore radius.

### 3.3 Molecular simulations and experimental data

We compared our MD simulations of pore conductance with experimental observations, specifically the single-pore KCl conductance obtained by the method of chronopotentiometry[26,28]. As Figure 5 shows, our simulated pore conductance is about twice the value extracted from chronopotentiometric experiments. Given the approximations of our ion models and the assumptions underlying the chronopotentiometric measurements, we consider this to be a reasonably close correspondence.

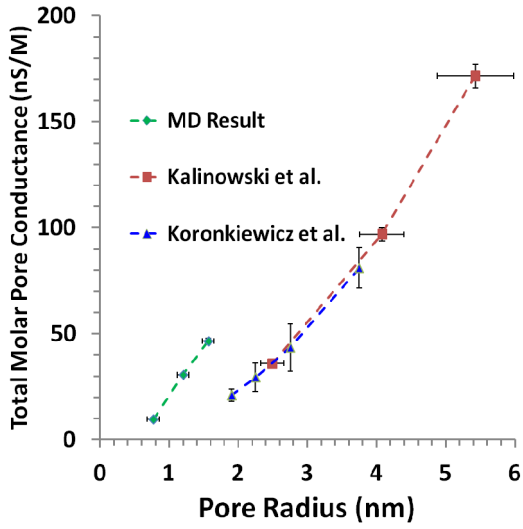


Figure 5. Comparison of simulated KCl conductance with chronopotentiometry data[26,28].

## 4. CONCLUSIONS

Simulations of phospholipid bilayers show that externally applied electric fields can cause the rearrangement of water and lipid molecules into a membrane-spanning pore of nanometer dimensions. At a more fundamental level we can describe this process as an electric-field driven re-ordering of water at the interface of bulk water and a low-permittivity

medium (vacuum or hydrocarbon) that leads to energy-minimized protrusions from the bulk water that facilitate the entry of water molecules into the low-permittivity medium. At the atomic scale the mechanism for this restructuring is stochastic thermal motion, biased by local electric field gradients.

Electrophoretic ion transport through field-stabilized lipid nanopores can be simulated using the methods of molecular dynamics. The radius of the electropore can be modulated over a range of 0.7 to 1.6 nm by varying the magnitude of the external electric field from 50 MV/m to 100 MV/m. Ion conductance is determined by two factors: pore radius and the extent of ion interaction with the phospholipid aqueous interface along the pore walls. The stronger binding of $Na^+$ results in significantly lower conductance for NaCl systems compared to KCl systems. This difference decreases as the pore radius is increased and the pore cross section becomes more and more dominated by bulk water, reducing the probability of pore wall interactions during transport. The electric conductance of a simulated electropore in a KCl-POPC system is comparable to the single-pore conductance extracted from chronopotentiometric measurements.

## REFERENCES


[1] E. Neumann, M. Schaefer-Ridder, Y. Wang *et al.*, "Gene transfer into mouse lyoma cells by electroporation in high electric fields," *EMBO J,* 1(7), 841-5 (1982).

[2] M. P. Rols, "Electropermeabilization, a physical method for the delivery of therapeutic molecules into cells," *Biochim Biophys Acta,* 1758, 423-428 (2006).

[3] U. Zimmermann, "Electric field-mediated fusion and related electrical phenomena," *Biochim. Biophys. Acta* 694(3), 227-277 (1982)

[4] M. Marty, G. Sersa, J. R. Garbay *et al.*, "Electrochemotherapy - An easy, highly effective and safe treatment of cutaneous and subcutaneous metastases: Results of ESOPE (European Standard Operating Procedures of Electrochemotherapy) study," *European Journal of Cancer Supplements,* 4(11), 3-13 (2006).

[5] R. Heller, M. J. Jaroszeski, L. F. Glass *et al.*, "Phase I/II trial for the treatment of cutaneous and subcutaneous tumors using electrochemotherapy," *Cancer,* 77(5), 964-71 (1996).

[6] B. Rubinsky, "Irreversible electroporation in medicine," *Technol Cancer Res Treat,* 6(4), 255-60 (2007).

[7] E. B. Garon, D. Sawcer, P. T. Vernier *et al.*, "In vitro and in vivo evaluation and a case report of intense nanosecond pulsed electric field as a local therapy for human malignancies," *Int J Cancer,* 121(3), 675-82 (2007).

[8] R. Nuccitelli, X. Chen, A. G. Pakhomov *et al.*, "A new pulsed electric field therapy for melanoma disrupts the tumor's blood supply and causes complete remission without recurrence," *Int J Cancer,* 125(2), 438-445 (2009).

[9] J. Teissie, M. Golzio, and M. P. Rols, "Mechanisms of cell membrane electropermeabilization: a minireview of our present (lack of ?) knowledge," *Biochim Biophys Acta,* 1724(3), 270-80 (2005).

[10] J. C. Weaver, and Y. A. Chizmadzhev, "Theory of electroporation: a review," *Bioelectrochemistry and Bioenergetics,* 41(2), 135-160 (1996).

[11] T. Kotnik, and D. Miklavcic, "Second-order model of membrane electric field induced by alternating external electric fields," *IEEE Trans Biomed Eng,* 47(8), 1074-81 (2000).

[12] R. Benz, and U. Zimmermann, "Pulse-length dependence of the electrical breakdown in lipid bilayer membranes," *Biochim Biophys Acta,* 597(3), 637-42 (1980).

[13] P. T. Vernier, Y. Sun, and M. A. Gundersen, "Nanoelectropulse-driven membrane perturbation and small molecule permeabilization," *BMC Cell Biology,* 7(1), 37 (2006).

[14] P. T. Vernier, Y. Sun, M. T. Chen *et al.*, "Nanosecond electric pulse-induced calcium entry into chromaffin cells," *Bioelectrochemistry,* 73(1), 1-4 (2008).

[15] S. Wang, J. Chen, M. T. Chen *et al.*, "Cardiac myocyte excitation by ultrashort high-field pulses," *Biophys J,* 96(4), 1640-1648 (2009).

[16] D. P. Tieleman, "The molecular basis of electroporation," *BMC Biochem,* 5(1), 10 (2004).

[17] P. T. Vernier, and M. J. Ziegler, "Nanosecond field alignment of head group and water dipoles in electroporating phospholipid bilayers," *J Phys Chem B,* 111(45), 12993-6 (2007).

[18] Z. A. Levine, and P. T. Vernier, "Life cycle of an electropore: field-dependent and field-independent steps in pore creation and annihilation," *J Membr Biol,* 236(1), 27-36 (2010).

[19] I. P. Sugar, and E. Neumann, "Stochastic model for electric field-induced membrane pores. Electroporation," *Biophys Chem,* 19(3), 211-25 (1984).

[20] K. A. DeBruin, and W. Krassowska, "Electroporation and shock-induced transmembrane potential in a cardiac fiber during defibrillation strength shocks," *Ann Biomed Eng,* 26(4), 584-96 (1998).

[21] S. A. Freeman, M. A. Wang, and J. C. Weaver, "Theory of electroporation of planar bilayer membranes: predictions of the aqueous area, change in capacitance, and pore-pore separation," *Biophys J,* 67(1), 42-56 (1994).
[22] R. W. Glaser, S. L. Leikin, L. V. Chernomordik *et al.*, "Reversible electrical breakdown of lipid bilayers: formation and evolution of pores," *Biochim Biophys Acta,* 940(2), 275-87 (1988).
[23] R. A. Bockmann, B. L. de Groot, S. Kakorin *et al.*, "Kinetics, statistics, and energetics of lipid membrane electroporation studied by molecular dynamics simulations," *Biophys J,* 95(4), 1837-50 (2008).
[24] T. J. Piggot, D. A. Holdbrook, and S. Khalid, "Electroporation of the *E. coli* and *S. aureus* membranes: molecular dynamics simulations of complex bacterial membranes," *J Phys Chem B,* 115(45), 13381-8 (2011).
[25] M. L. Fernandez, M. Risk, R. Reigada *et al.*, "Size-controlled nanopores in lipid membranes with stabilizing electric fields," *Biochem Biophys Res Commun,* 423(2), 325-30 (2012).
[26] S. Kalinowski, G. Ibron, K. Bryl *et al.*, "Chronopotentiometric studies of electroporation of bilayer lipid membranes," *Biochim Biophys Acta,* 1369(2), 204-12 (1998).
[27] S. Koronkiewicz, S. Kalinowski, and K. Bryl, "Programmable chronopotentiometry as a tool for the study of electroporation and resealing of pores in bilayer lipid membranes," *Biochim Biophys Acta,* 1561(2), 222-9 (2002).
[28] S. Koronkiewicz, and S. Kalinowski, "Influence of cholesterol on electroporation of bilayer lipid membranes: chronopotentiometric studies," *Biochim Biophys Acta,* 1661(2), 196-203 (2004).
[29] Z. A. Levine, and P. T. Vernier, "Calcium and phosphatidylserine inhibit lipid electropore formation and reduce pore lifetime," *J Membr Biol,* 245(10), 599-610 (2012).
[30] Y. Okuno, M. Minagawa, H. Matsumoto *et al.*, "Simulation study on the influence of an electric field on water evaporation," *Journal of Molecular Structure: THEOCHEM,* 904(1-3), 83-90 (2009).